

Wilson loops from multicentre and rotating branes, mass gaps and phase structure in gauge theories

A. Brandhuber and K. Sfetsos

Theory Division, CERN
CH-1211 Geneva 23, Switzerland
brandhu,sfetsos@mail.cern.ch

Abstract

Within the AdS/CFT correspondence we use multicentre D3-brane metrics to investigate Wilson loops and compute the associated heavy quark–antiquark potentials for the strongly coupled $SU(N)$ super-Yang–Mills gauge theory, when the gauge symmetry is broken by the expectation values of the scalar fields. For the case of a uniform distribution of D3-branes over a disc, we find that there exists a maximum separation beyond which there is no force between the quark and the antiquark, i.e. the screening is complete. We associate this phenomenon with the possible existence of a mass gap in the strongly coupled gauge theory. In the finite-temperature case, when the corresponding supergravity solution is a rotating D3-brane solution, there is a class of potentials interpolating between a Coulombic and a confining behaviour. However, above a certain critical value of the mass parameter, the potentials exhibit a behaviour characteristic of statistical systems undergoing phase transitions. The physical path preserves the concavity property of the potential and minimizes the energy. Using the same rotating-brane solutions, we also compute spatial Wilson loops, associated with the quark–antiquark potential in models of three-dimensional gauge theories at zero temperature, with similar results.

1 Introduction

The study of $\mathcal{N} = 4$ $SU(N)$ Yang–Mills (SYM) gauge theory, at large N and for large 't Hooft coupling constant $R^4 = 4\pi g_{\text{YM}}^2 N$, is based, in the supergravity approach, on the type-IIB supergravity solution representing N coincident D3-branes. The metric is

$$ds^2 = H^{-1/2}(-dt^2 + dy_1^2 + dy_2^2 + dy_3^2) + H^{1/2}(dx_1^2 + \dots + dx_6^2) , \quad (1)$$

where the harmonic function parametrizing the solution is given by

$$H = 1 + \frac{R^4 \alpha'^2}{r^4} , \quad r^2 \equiv x_1^2 + x_2^2 + \dots + x_6^2 . \quad (2)$$

The constant string coupling is $e^\Phi = g_s = g_{\text{YM}}^2$ and we have omitted the self-dual five-form. The field theory correspondence [1, 2, 3] is obtained by going to the near-horizon limit

$$U = \frac{r}{\alpha'} , \quad U_i = \frac{x_i}{\alpha'} , \quad i = 1, 2, \dots, 6 , \quad \alpha' \rightarrow 0 , \quad (3)$$

where the metric factorizes as $AdS_5 \times S^5$ with both factors having equal radii $R\sqrt{\alpha'}$. When the $SU(N)$ gauge symmetry is broken by non-zero expectation values (vev's) for the scalar fields, then the appropriate supergravity solution has a metric given by (1), but with the single-centre harmonic function (2) replaced by the multicentre one

$$H = 1 + 4\pi g_s \alpha'^2 \sum_{i=1}^N \frac{c_i}{|\mathbf{x} - \mathbf{x}_i|^4} , \quad \sum_{i=1}^N c_i = N , \quad (4)$$

while the dilaton remains constant.

In the AdS/CFT correspondence, isometries of the background are identified with global symmetries of the gauge theory. A generic choice of vectors \mathbf{x}_i completely breaks the $SU(4) \simeq SO(6)$ \mathcal{R} -symmetry of the theory. However, in this paper we consider cases where the \mathcal{R} symmetry group is only partially broken to $SO(4)$ times a discrete subgroup. This is achieved by placing the D3-branes in a plane lying in the six-dimensional space transverse to the D3-branes. It is worth mentioning that in the field theory limit (3) there is no supersymmetry enhancement since the (super)conformal invariance is broken by any non-zero vev's and only $\mathcal{N} = 4$ super-Poincaré invariance remains. An important question is whether there exist supergravity descriptions of the same theories with broken gauge group at finite temperature. The corresponding solutions must be non-extremal versions of the backgrounds corresponding to multicentre metrics. The construction of such solutions is in general not possible since, at non-extremality, the gravitational attraction of the non-BPS branes is no longer balanced by their RR-repulsion. However, this is possible when we are dealing with rotating D3-brane solutions [4, 5, 6, 7], when the attractive forces are balanced by centrifugal forces. In this paper we will use a class of such solutions, which has one rotation parameter [5] that breaks the \mathcal{R} -symmetry $SO(6)$ of (1) with (2), to an $SO(4) \times U(1)$ subgroup. In this case the extremal limit of the solution describes a uniform distribution of D3-branes over a disc [6, 8].

In this paper we are interested in computing the quark–antiquark potential using rotating D3-branes, since multicentre supersymmetric D3-brane solutions, with a continuous distribution for the branes, arise when the extremal limit is taken. In order to calculate the quark–antiquark potential we use a method introduced by [9, 10]. According to this prescription the expectation value of a Wilson loop of the field theory living on the boundary is given by the partition function of a fundamental string in the relevant background and fixed on the boundary to the contour of the Wilson loop that is to be calculated. In principle this amounts to summing over all possible surfaces of arbitrary genus with the given boundary conditions and all quantum fluctuations. In the supergravity approximation, which is valid for large 't Hooft coupling, $R^4 = 4\pi N g_{YM}^2$, the problem reduces to finding the minimal area surface that ends on the contour of the Wilson loop on the boundary. The Wilson loop calculated using this procedure deviates from the usual definition of Wilson loops in that it includes the adjoint scalar fields (and the fermions). This can be understood as follows: in string theory, an external quark (or antiquark) is represented as an open string stretched from the horizon (location of the D3-branes) to the boundary of the AdS space. Since the string “pulls” the D3-branes, these are deformed, which amounts to turning on scalar fields of the world–volume theory on the branes. Along the Wilson loop the scalars can take non-trivial paths in all six transverse directions, but in the following we will consider Wilson loops for which only the scalar corresponding to the radial coordinate U is active and the others are chosen to be constant.

To be more specific, we have to minimize the Nambu–Goto action of a fundamental string in the relevant supergravity background. In order to calculate the potential between a quark and an antiquark, we take a rectangular loop on the boundary with one side of length L in the space direction and one of length \mathcal{T} in the (Euclidean) time direction, as in field theory. Since the configuration is static, the time integration trivially yields a factor of \mathcal{T}

$$S_{NG} = \frac{\mathcal{T}}{2\pi\alpha'} \int dy \sqrt{g(U) \left(\frac{dU}{dy} \right)^2 + f(U)/R^4}, \quad (5)$$

where $g(U) = g_{\tau\tau}g_{UU}$ and $f(U) = R^4 g_{\tau\tau}g_{yy}$, for supersymmetric theories at zero and finite temperature (section 2 and 3). In section 4, where we study supergravity duals of non-supersymmetric gauge theories, one of the spatial coordinates, say y_1 , is taken as the Euclidean time and, hence, $g(U) = g_{yy}g_{UU}$ and $f(U) = R^4 g_{yy}^2$.

The integrals for the length and energy of the Wilson loop, respectively, are computed using standard methods developed in [10, 9]. They are given by

$$L = 2R^2 \sqrt{f(U_0)} \int_{U_0}^{\infty} dU \sqrt{\frac{g(U)}{f(U)(f(U) - f(U_0))}}, \quad (6)$$

and

$$E_{q\bar{q}} = \frac{1}{\pi} \int_{U_0}^{\infty} dU \left[\sqrt{\frac{g(U)f(U)}{f(U) - f(U_0)}} - \sqrt{g(U)} \right] - \frac{1}{\pi} \int_{U_{\min}}^{U_0} dU \sqrt{g(U)}, \quad (7)$$

where U_0 denotes the lowest value of U that can be reached by a certain string geodesic, and U_{\min} is the minimal U_0 allowed by the physics and the geometry of the particular application. This could be the radius of the disc in the case of the corresponding multicentre metric or the horizon in the case of non-zero temperature. Note that we have chosen the arbitrary constant that may be added to the energy given by (7), in such a way that the energy of a non-interacting pair of quark and antiquark is zero. From the form of the multicentre harmonic (4) it is clear that our multicentre metrics approach, for large U , the metric corresponding to $AdS_5 \times S^5$ and the same would also be true for the rotating brane solutions. In the conformal case [9, 10] we have $f(U) = U^4$, $g(U) = 1$, $U_{\min} = 0$ and we find for the length

$$L = \frac{2\sqrt{\pi}\Gamma(3/4)R^2}{\Gamma(1/4)U_0}, \quad (8)$$

and for the energy

$$\begin{aligned} E_{q\bar{q}} &= -\frac{\Gamma(3/4)}{\sqrt{\pi}\Gamma(1/4)}U_0 \\ &= -\frac{2\Gamma(3/4)^2R^2}{\Gamma(1/4)^2} \frac{1}{L}. \end{aligned} \quad (9)$$

One of the issues that we will investigate in detail in section 3 and 4 is whether the concavity condition on the potential of a heavy quark–antiquark pair

$$\frac{dE_{q\bar{q}}}{dL} > 0, \quad (10)$$

$$\frac{d^2E_{q\bar{q}}}{dL^2} \leq 0, \quad (11)$$

is obeyed. In physical terms, (10) and (11) mean that the force between the quark and the antiquark is always attractive and a non-increasing function of their separation distance. These conditions were proved in general in [11], building on work in [12]. Hence, they should be satisfied by the potentials computed using the AdS/CFT correspondence at any order of approximation and in particular in the supergravity approximation. Using (6) and (7) we find that

$$\frac{dE_{q\bar{q}}}{dL} = \frac{\sqrt{f(U_0)}}{2\pi R^2} > 0, \quad (12)$$

$$\frac{d^2E_{q\bar{q}}}{dL^2} = \frac{1}{4\pi R^2} \frac{f'(U_0)}{\sqrt{f(U_0)}} \frac{1}{L'(U_0)}, \quad (13)$$

where the prime denotes a derivative with respect to U_0 . Hence, the force remains always attractive, except at the point where $f(U_0) = 0$ and (10) is always satisfied. However, the concavity condition (11) might fail since, even though in all of our examples $f'(U_0) > 0$, there can be occasions where $L'(U_0)$ changes sign.¹ We will see that such behaviour

¹This, apparently, is in conflict with theorem 1 in [13]. Given the explicit nature of our calculations in sections 3 and 4, it seems that the validity of this theorem be restricted for $E_{q\bar{q}} < 0$.

occurs only on non-physical branches of the potential and was already encountered in previous examples [14, 15]. We also note that, because of (12), L and $E_{q\bar{q}}$ reach their extrema at the same value of U_0 .

The paper is organized as follows: in section 2 we study Wilson loops in $\mathcal{N} = 4$ SYM with broken gauge symmetry, using the background for D3-branes uniformly distributed on a disc. We show that there is a screening behaviour such that the potential vanishes at a finite distance. We argue that this signals the existence of a mass gap in the theory at strong coupling. In section 3 we consider Wilson loops in $\mathcal{N} = 4$ SYM at finite temperature, using rotating D3-brane solutions and work out the phase structure in detail. In section 4 we use the same rotating D3-brane backgrounds to study non-supersymmetric gauge theories in three dimensions; as expected, we find confinement, but also a phase transition, depending on the ratio of the mass to the rotation parameter. We present our conclusions and some open problems in section 5. We have also written an appendix, where we briefly discuss Wilson loops obtained using the background for D3-branes distributed uniformly on the circumference of a ring.

2 D3-branes distributed on a disc

As our first example we consider N D3-branes distributed, uniformly in the angular direction, inside a disc of radius r_0 in the x_5 - x_6 plane. Their centres are given by [8]

$$\begin{aligned} \mathbf{x}_{ij} &= (0, 0, 0, 0, r_{0j} \cos \phi_i, r_{0j} \sin \phi_i) , \\ \phi_i &= \frac{2\pi i}{\sqrt{N}} , \quad r_{0j} = r_0 \left(j/\sqrt{N} \right)^{1/2} , \quad i, j = 0, 1, \dots, \sqrt{N} - 1 , \end{aligned} \quad (14)$$

and uniformity of the distribution means that we take the constants c_i appearing in (4) equal to 1. Since we are interested in the large- N limit, we may take $\sqrt{N} = \text{integer}$ without loss of generality. For a number of D3-branes, $N \gg 1$ and in the field theory limit (3), where in addition we keep finite the energy of strings stretched between D3-branes situated at the centres by rescaling $r_0 \rightarrow \alpha' r_0$, we may replace the sum by an integral; the metric then takes the form (1) with harmonic given by [8]

$$\begin{aligned} H &= \frac{2R^4/\alpha'^2}{\sqrt{(U^2 + r_0^2)^2 - 4r_0^2 u^2} \left(U^2 - r_0^2 + \sqrt{(U^2 + r_0^2)^2 - 4r_0^2 u^2} \right)} \\ U^2 &= U_1^2 + \dots + U_6^2 , \quad u^2 = U_5^2 + U_6^2 . \end{aligned} \quad (15)$$

It is easy to see that the above harmonic is indeed singular inside a disc of radius r_0 in the x_5 - x_6 plane. This distribution of D3-branes is what is obtained [6, 8] in the extremal limit of the D3-brane rotating solution with one rotation parameter of [5].

2.1 Trajectory orthogonal to the disc

There are two simple trajectories we use to investigate the quark–antiquark potential. First consider the trajectory in the hyperplane defined by

$$x_5 = x_6 = 0, \quad u = 0, \quad (16)$$

that is along an axis passing through the centre of the disc. In that case we have

$$f(U) = U^2(U^2 + r_0^2), \quad g(U) = 1 \quad (17)$$

and the minimum value for U_0 is $U_{\min} = 0$. The expression for the length as a function of U_0 is given by (we change the integration variable in (6) and (7) as $\rho = U^2$)²

$$\begin{aligned} L &= R^2 U_0 \sqrt{r_0^2 + U_0^2} \int_{U_0^2}^{\infty} \frac{d\rho}{\rho \sqrt{(\rho + r_0^2)(\rho - U_0^2)(\rho + r_0^2 + U_0^2)}} \\ &= \frac{2R^2 U_0 k'}{U_0^2 + r_0^2} (\mathbf{\Pi}(k'^2, k) - \mathbf{K}(k)), \end{aligned} \quad (18)$$

whereas for the quark–antiquark potential as a function of U_0 , we obtain

$$\begin{aligned} E_{q\bar{q}} &= \frac{1}{2\pi} \int_{U_0^2}^{\infty} d\rho \left[\sqrt{\frac{\rho + r_0^2}{(\rho - U_0^2)(\rho + r_0^2 + U_0^2)}} - \frac{1}{\sqrt{\rho}} \right] - \frac{U_0}{\pi} \\ &= \frac{\sqrt{2U_0^2 + r_0^2}}{\pi} (k'^2 \mathbf{K}(k) - \mathbf{E}(k)), \end{aligned} \quad (19)$$

with $k = \frac{U_0}{\sqrt{r_0^2 + 2U_0^2}}$ and $k' = \sqrt{1 - k^2}$. For the disc metric we find Coulombic behaviour for small L , as expected, but an expansion of the integrals for small U_0 reveals a quite different behaviour for larger values of L . We find that

$$L = \frac{\pi R^2}{r_0} \left(1 - \frac{U_0}{r_0} \right) + \mathcal{O}(U_0^2) \quad (20)$$

and

$$E_{q\bar{q}} = -\frac{U_0^2}{4r_0} + \mathcal{O}(U_0^4). \quad (21)$$

Hence, we see that there exists a maximum length

$$L_{\max} = \frac{\pi R^2}{r_0}, \quad (22)$$

after which there is no force to keep the quark and antiquark together. Solving for U_0 in terms of L , using (20), we find that

$$E_{q\bar{q}} = -\frac{r_0^3}{4} \left(\frac{L_{\max} - L}{\pi R^2} \right)^2 \Theta(L_{\max} - L) + \mathcal{O}(L_{\max} - L)^4, \quad (23)$$

²In what follows $\mathbf{K}(k)$, $\mathbf{E}(k)$ and $\mathbf{\Pi}(n, k)$ are complete integrals of the first, second and third kind, respectively. In this paper we follow the conventions of [16, 17].

where the step function $\Theta(L_{\max} - L)$ enforces the maximum length condition. The potential goes to zero for a finite separation L_{\max} , which corresponds to a trajectory that goes all the way down to $U = 0$ i.e. touches the disc.

The heavy quark–antiquark potential energy as a function of the separation is depicted by curve (b) in fig. 1.

2.2 Trajectory lying on the plane of the disc

For the trajectory along an axis that lies on the plane of the disc and goes through its centre, we have

$$x_1 = x_2 = x_3 = x_4 = 0, \quad U = u \quad (24)$$

and

$$f(U) = (U^2 - r_0^2)^2, \quad g(U) = 1, \quad (25)$$

whereas $U_{\min} = r_0$. The latter condition means that no trajectory can penetrate the disc. After we change the integration variable as $\rho = U^2$ the integral (6) for the length becomes

$$L = R^2(U_0^2 - r_0^2) \int_{U_0^2}^{\infty} \frac{d\rho}{(\rho - r_0^2)\sqrt{\rho(\rho - U_0^2)(\rho + U_0^2 - 2r_0^2)}}. \quad (26)$$

Similarly, that of the quark–antiquark potential in (7) becomes

$$E_{q\bar{q}} = \frac{1}{2\pi} \int_{U_0^2}^{\infty} d\rho \left(\frac{\rho - r_0^2}{\sqrt{\rho(\rho - U_0^2)(\rho + U_0^2 - 2r_0^2)}} - \frac{1}{\sqrt{\rho}} \right) - \frac{U_0 - r_0}{\pi}. \quad (27)$$

They can be written in terms of elliptic integrals of the first and the third kind as

$$L = \left\{ \begin{array}{ll} \frac{2R^2(U_0^2 - r_0^2)}{r_0^2 U_0} \left(\mathbf{\Pi}(r_0^2/U_0^2, k_1) - \mathbf{K}(k_1) \right) & \text{if } r_0^2 \leq U_0^2 \leq 2r_0^2 \\ \frac{\sqrt{2}R^2}{\sqrt{U_0^2 - r_0^2}} \left(\mathbf{\Pi}(\frac{1}{2}, k_2) - \mathbf{K}(k_2) \right) & \text{if } U_0^2 \geq 2r_0^2 \end{array} \right\}, \quad (28)$$

and

$$E_{q\bar{q}} = \left\{ \begin{array}{ll} -\frac{U_0}{2\pi}(1 + k_1)\mathbf{E}\left(\frac{2\sqrt{k_1}}{1+k_1}\right) + \frac{r_0}{\pi} & \text{if } r_0^2 \leq U_0^2 \leq 2r_0^2 \\ \frac{\sqrt{U_0^2 - r_0^2}}{\sqrt{2}\pi} \left(\mathbf{K}(k_2) - 2\mathbf{E}(k_2) \right) + \frac{r_0}{\pi} & \text{if } U_0^2 \geq 2r_0^2 \end{array} \right\}, \quad (29)$$

where $k_1 = \frac{\sqrt{2r_0^2 - U_0^2}}{U_0}$ and $k_2 = \sqrt{\frac{U_0^2 - 2r_0^2}{2U_0^2 - 2r_0^2}}$. It can be checked that L and $E_{q\bar{q}}$, as given by (28) and (29), are smooth functions at $U_0 = \sqrt{2}r_0$. The behaviour is similar to that in the previous case. We find³

$$L = \frac{\pi R^2}{2r_0} \left(1 - \frac{2(U_0 - r_0)}{r_0} \left(\ln \left(\frac{4r_0}{U_0 - r_0} \right) - 1 \right) \right) + \mathcal{O}(U_0 - r_0)^2, \quad (30)$$

³The expansion of the complete elliptic integral of the third kind $\mathbf{\Pi}(r_0^2/U_0^2, k_1)$ is facilitated if it is first expressed in terms of (incomplete) integrals of the first and second kind, using eq. 412.01 of [17].

and

$$E_{q\bar{q}} = -\frac{(U_0 - r_0)^2}{2\pi r_0} \left(\ln \left(\frac{4r_0}{U_0 - r_0} \right) - \frac{3}{2} \right) + \mathcal{O}(U_0 - r_0)^4, \quad (31)$$

and hence there is a screening behaviour. The maximal separation of the quark–antiquark pair is

$$L_{\max} = \frac{\pi R^2}{2r_0}. \quad (32)$$

The heavy quark–antiquark potential energy as a function of the separation is depicted by curve (a) in fig. 1.

2.3 The mass gap

We have seen that in both cases there exists a maximum length at which the force between the quark and antiquark becomes zero, i.e. complete screening! For a separation of the quark–antiquark pair $L > L_{\max}$ we do not find a geodesic connecting them and the solution is given by two straight strings corresponding to zero potential and zero force between the quark and the antiquark. The latter state is in fact the physical one and prevents a violation of the condition (10). A screening-type behaviour is typical of Wilson loops at finite temperature [15] and also in theories at zero temperature, with running YM coupling constant [18] (because of non-constant dilaton), but it was not expected for a theory at zero temperature with constant dilaton. From a physical point of view the existence of a maximum length $L_{\max} \sim \frac{R^2}{r_0}$ means that one cannot probe at arbitrarily small energy scales. This is a signal that the gauge theory at strong coupling exhibits a mass gap $M_{\text{gap}} \sim \frac{r_0}{R^2}$. In order to investigate this we start with the massless wave equation

$$\frac{1}{\sqrt{G}} \partial_\mu \sqrt{G} G^{\mu\nu} \partial_\nu \Psi = 0. \quad (33)$$

We make the ansatz $\Psi = \phi(U) e^{ik \cdot y}$ and define the (mass)² as $M^2 = -k^2$ in the spirit of [19]. In the background (15) we obtain the following second order differential equation⁴ for $\phi(U)$

$$\partial_U U^3 (U^2 + r_0^2) \partial_U \phi + R^4 M^2 U \phi = 0, \quad (34)$$

whose general solution, for $q \neq 0$, can be written in terms of hypergeometric functions as

$$\begin{aligned} \phi &= C_1 \left(\frac{r_0}{U} \right)^{1+q} F \left(-\frac{1+q}{2}, \frac{3-q}{2}, 1-q; -(U/r_0)^2 \right) \\ &\quad + C_2 \left(\frac{r_0}{U} \right)^{1-q} F \left(-\frac{1-q}{2}, \frac{3+q}{2}, 1+q; -(U/r_0)^2 \right), \quad (35) \\ q &\equiv \sqrt{1 - R^4 M^2 / r_0^2}, \end{aligned}$$

where C_1, C_2 are constant coefficients. The solution that is valid for $q = 0$ can also be written down using [16, 20], but it will not be needed for our purposes. Depending on

⁴The coordinate U appearing in this subsection is not the same as the one in (15). The two are related by the coordinate transformation (50), relating (51) to (40), if we analytically continue $r_0^2 \rightarrow -r_0^2$.

the value of M , the parameter q is real or purely imaginary. We will show that only in the latter case may we obtain a basis that is orthonormalizable in the Dirac sense (with the use of a δ -function) with measure dUU . Indeed, the behaviour of (35) for small U is

$$\phi \simeq C_1 \left(\frac{r_0}{U}\right)^{1+q} + C_2 \left(\frac{r_0}{U}\right)^{1-q}, \quad \text{as } U \rightarrow 0^+. \quad (36)$$

Hence, if q is real, the orthonormalizability condition requires that $C_1 = 0$. On the other hand if q is imaginary, the reality condition requires that C_1 and C_2 be complex conjugate to each other. Similarly the behaviour of (35) for large U is

$$\begin{aligned} \phi \simeq & C_1 \frac{\Gamma(1-q)}{\Gamma(3/2-q/2)^2} + C_2 \frac{\Gamma(1+q)}{\Gamma(3/2+q/2)^2} + \frac{R^8 M^4}{32U^4} \\ & \times \left[C_1 \frac{\Gamma(1-q)}{\Gamma(3/2-q/2)^2} \left(2 \ln \left(\frac{U}{r_0} \right) + \frac{3}{2} - 2\gamma - \frac{4r_0^2}{R^4 M^2} - 2\Psi \left(\frac{1-q}{2} \right) \right) \right. \\ & \left. + C_2 \frac{\Gamma(1+q)}{\Gamma(3/2+q/2)^2} \left(2 \ln \left(\frac{U}{r_0} \right) + \frac{3}{2} - 2\gamma - \frac{4r_0^2}{R^4 M^2} - 2\Psi \left(\frac{1+q}{2} \right) \right) \right], \end{aligned} \quad (37)$$

as $U \rightarrow \infty$,

where γ is Euler's constant and $\Psi(z) = \frac{d \ln \Gamma(z)}{dz}$ is the so-called psi function.⁵ It is clear that orthonormalizability requires that the constant term in the above expansion vanishes, giving

$$C_1 \frac{\Gamma(1-q)}{\Gamma(3/2-q/2)^2} + C_2 \frac{\Gamma(1+q)}{\Gamma(3/2+q/2)^2} = 0. \quad (38)$$

As we have mentioned, real q requires that $C_1 = 0$ and, because of (38), $C_2 = 0$ as well. Hence, the only possibility to have square integrable solutions is to require an imaginary q . Indeed, (37) then behaves as $1/U^4$ for large values of U . Furthermore, the condition that q is imaginary leads to a mass gap

$$M_{\text{gap}} = \frac{r_0}{R^2}, \quad (39)$$

which is of the order expected from the quark–antiquark potential computations. The mass spectrum above the mass gap is continuous.

3 Rotating D3-brane solution

A rotating D3-brane solution of type-IIB supergravity was found in [5] (based on [4]). For our purposes we pass to the Euclidean regime, where the time variable as well as the angular parameter are analytically continued. In the field theory limit, the metric is

⁵In finding the asymptotic behaviours in (36) and (37), we have used the fact that $F(a, b, c; 0) = 1$, the relation 15.3.14 of [20], as well as some properties of the psi function.

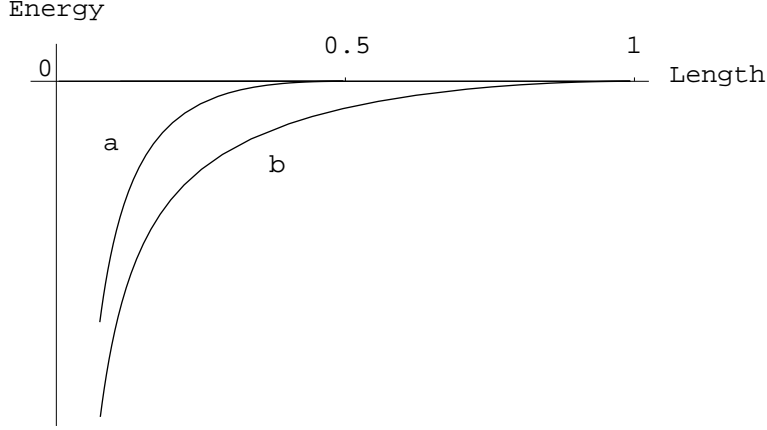


Figure 1: Curve (a) corresponds to the quark–antiquark potential as computed using (28) and (29). Curve (b) corresponds to the same potential as computed using (18) and (19). Lengths and energies are measured in units of $\frac{\pi R^2}{r_0}$ and r_0 , respectively. Both curves demonstrate that there is a maximum value L_{\max} , given by (32) and (22), where the energy becomes zero and the screening of charges is complete.

therefore given by (the dilaton is constant and we omit the self-dual five-form):

$$\begin{aligned}
 ds^2 = & H^{-1/2} (f d\tau^2 + dy_1^2 + dy_2^2 + dy_3^2) + \alpha'^2 H^{1/2} \left(\frac{dU^2}{f_1} + (U^2 - r_0^2 \cos^2 \theta) d\theta^2 \right. \\
 & \left. + (U^2 - r_0^2) \sin^2 \theta d\phi^2 + U^2 \cos^2 \theta d\Omega_3^2 - \frac{2\mu^2 r_0}{R^2} \sin^2 \theta d\tau d\phi \right), \quad (40)
 \end{aligned}$$

with

$$\begin{aligned}
 H &= \frac{R^4/\alpha'^2}{U^2(U^2 - r_0^2 \cos^2 \theta)}, \\
 f &= 1 - \frac{\mu^4}{U^2(U^2 - r_0^2 \cos^2 \theta)}, \\
 f_1 &= \frac{U^4 - r_0^2 U^2 - \mu^4}{U^2(U^2 - r_0^2 \cos^2 \theta)},
 \end{aligned} \quad (41)$$

where r_0 is the “Euclidean” angular momentum parameter. The location of the horizon is given by the positive root of the equation $U^4 - r_0^2 U^2 - \mu^4 = 0$:

$$U_H^2 = \frac{1}{2} \left(r_0^2 + \sqrt{r_0^4 + 4\mu^4} \right), \quad (42)$$

whereas the temperature associated with (40) is

$$T_H = \frac{U_H}{2\pi R^2 \mu^2} \sqrt{r_0^4 + 4\mu^4}. \quad (43)$$

Using the expression for the curvature-invariant $R_{\mu\nu}R^{\mu\nu}$ as given by eq. (3.21) of [5] (analytically continued in the Euclidean regime), we see that the metric (40) has singularities, at $U = 0$ and at $U^2 = r_0^2 \cos^2 \theta$, which are hidden inside the horizon at $U = U_H$, provided that $\mu > 0$.

In this section we are interested in calculating the potential between a quark and an antiquark in a four-dimensional gauge theory at finite temperature.⁶ At finite temperature the time coordinate is periodically identified and the rectangular Wilson loop at zero temperature is wrapped on the time direction. Therefore the topology of the boundary of the Wilson loop at finite temperature is that of two circles separated in the space direction by a distance L . On the supergravity side this means that we have to minimize the area of a cylindrical string ending on two cycles at the boundary. Since the configuration is time-independent, formulae (5)–(7) can be used without modification to calculate the quark–antiquark potential.

3.1 Finite temperature and zero rotation

Before we examine the general case in detail we focus our attention to two particular limits, where the metric (40) simplifies considerably and we may compute the integrals in (6) and (7) explicitly. In the first, the parameter $r_0 \ll \mu$. Then we obtain the non-extremal D3-brane metric in the field theory limit given by

$$ds^2 = \frac{U^2}{R^2} \left(\left(1 - \frac{\mu^4}{U^4}\right) d\tau^2 + dy_1^2 + dy_2^2 + dy_3^2 \right) + \frac{R^2}{U^2} \left(\left(1 - \frac{\mu^4}{U^4}\right)^{-1} dU^2 + U^2 d\Omega_5^2 \right). \quad (44)$$

Wilson loops in this background were studied in [14, 15]. Here we show that various results can be expressed in terms of hypergeometric functions. We have

$$f(U) = U^4 - \mu^4, \quad g(U) = 1 \quad (45)$$

and $U_{\min} = \mu$. Using (6) and (7), we find for the length:

$$\begin{aligned} L &= 2R^4 \sqrt{U_0^4 - \mu^4} \int_{U_0}^{\infty} \frac{dU}{\sqrt{(U^4 - \mu^4)(U^4 - U_0^4)}} \\ &= \frac{1}{2} B(3/4, 1/2) \frac{R^2}{U_0} \sqrt{1 - \mu^4/U_0^4} F\left(\frac{1}{2}, \frac{3}{4}, \frac{5}{4}; \mu^4/U_0^4\right) \end{aligned} \quad (46)$$

and for the energy:

$$\begin{aligned} E_{q\bar{q}} &= \frac{1}{\pi} \int_{U_0}^{\infty} dU \left(\sqrt{\frac{U^4 - \mu^4}{U^4 - U_0^4}} - 1 \right) - \frac{U_0 - \mu}{\pi} \\ &= \frac{B(-1/4, 1/2)}{4\pi} U_0 F\left(-\frac{1}{2}, -\frac{1}{4}, \frac{1}{4}; \mu^4/U_0^4\right) + \frac{\mu}{\pi}. \end{aligned} \quad (47)$$

⁶For a pedagogical review of gauge theories at finite temperature, see [21].

For $U_0 \gg \mu$ we have the usual Coulombic behaviour, and the potential is given by (9). As U_0 decreases to $U_0 \simeq 1.18\mu$ the length and energy reach their maximum values $L_{\max} \simeq 0.87R^2/\mu$ and $E_{q\bar{q}}^{\max} \simeq 0.03\mu$. However, before that, for $U_0 \simeq 1.52\mu$ the energy turns positive and the corresponding value for the length is $L \simeq 0.75R^2/\mu$. As $U_0 \rightarrow \mu$ we find that both the length and the energy approach zero as⁷

$$L \simeq \frac{R^2}{\mu} \sqrt{\frac{U_0}{\mu} - 1} \left(\ln \left(\frac{128\mu}{U_0 - \mu} \right) - \frac{\pi}{2} \right), \quad (48)$$

and

$$E_{q\bar{q}} \simeq \frac{U_0 - \mu}{2\pi} \left(\ln \left(\frac{128\mu}{U_0 - \mu} \right) - 1 - \frac{\pi}{2} \right). \quad (49)$$

The plots of the length and potential as functions of U_0 and that of the potential as a function of the length are given by curve (c) in figs. 2, 3 and 4.

3.2 The supersymmetric limit and a multicentre metric

A second interesting limit is the extremal limit corresponding to $r_0 \gg \mu$, where the solution becomes supersymmetric. In this case (strictly speaking exactly for $\mu = 0$) the part of the singularity surface at $U^2 = r_0^2 \cos^2 \theta$ corresponding to $\theta = 0$ coincides with the location of the would-be horizon, which, using (42), is easily seen to be at $U_H = r_0$. The nature of this surface, where there will be a distribution of D3-branes, becomes transparent after the change of variables (valid for the region $U_0 \geq r_0$)

$$\begin{aligned} \begin{pmatrix} x_1 \\ x_2 \end{pmatrix} &= U \cos \theta \sin \psi \begin{pmatrix} \cos \phi_1 \\ \sin \phi_1 \end{pmatrix}, \\ \begin{pmatrix} x_3 \\ x_4 \end{pmatrix} &= U \cos \theta \cos \psi \begin{pmatrix} \cos \phi_2 \\ \sin \phi_2 \end{pmatrix}, \\ \begin{pmatrix} x_5 \\ x_6 \end{pmatrix} &= \sqrt{U^2 - r_0^2} \sin \theta \begin{pmatrix} \cos \phi \\ \sin \phi \end{pmatrix}, \end{aligned} \quad (50)$$

where ψ , ϕ_1 and ϕ_2 parametrize the line element $d\Omega_3^2$ for S^3 , and we find

$$\begin{aligned} ds^2 &= H^{-1/2} (d\tau^2 + dy_1^2 + dy_2^2 + dy_3^2) + H^{1/2} (dx_1^2 + \dots + dx_6^2), \\ H &= \frac{2R^4/\alpha'^2}{\sqrt{(U^2 - r_0^2)^2 + 4r_0^2 u^2} \left(U^2 + r_0^2 + \sqrt{(U^2 - r_0^2)^2 + 4r_0^2 u^2} \right)}, \\ U^2 &= x_1^2 + \dots + x_6^2, \quad u^2 = x_5^2 + x_6^2. \end{aligned} \quad (51)$$

⁷In the absence of the logarithmic dependence in (48) and (49) the potential energy would have gone to zero as L^2 for small separations. Owing to the presence of logarithm, it is not possible to find the analytic expression of the potential energy as a function of the length, even if this is small. Nevertheless we easily deduce that it goes to zero faster than L^2 . The authors of [14] have presented a power-law behaviour of the type $L^{3.6}$ based on numerical fitting.

Notice the symbol U in (50) and (51) refers to two different coordinates. The above harmonic function can be obtained from (15) if we analytically continue $r_0 \rightarrow -ir_0$. This continuation changes the singularity structure of the harmonic function. It no longer represents D3-branes uniformly distributed over a disc of radius r_0 at the x_5-x_6 plane, but rather D3-branes uniformly distributed over a 3-sphere defined by $x_1^2+x_2^2+x_3^2+x_4^2 = r_0^2$ and $x_5 = x_6 = 0$. Notice that the location of the singularity coincides with that of the would-be horizon and therefore it is meaningless to talk about Hawking temperature in this case (note that the expression for T_H in (43) diverges in the limit $\mu \rightarrow 0$).

Before we actually compute the Wilson loops associated with the supersymmetric limit, let us show that even in that limit there exists a mass gap and, hence, we expect screening. As before we start with the massless wave equation (33), with the same ansatz $\Psi = \phi(U)e^{ik \cdot y}$ and definition of the (mass)² as $M^2 = -k^2$. Then we obtain a second order linear differential equation for $\phi(U)$, which, after changing variables as

$$\phi = (1-z)^2 Y(z) , \quad z = 1 - \frac{2r_0^2}{U^2} , \quad |z| \leq 1 , \quad (52)$$

becomes

$$(1-z^2)Y'' - 2(1+2z)Y' + \left(\frac{R^4 M^2}{4r_0^2} - 2 \right) Y = 0 , \quad (53)$$

which is the Jacobi equation. This has a complete set of normalizable solutions in terms of the Jacobi polynomials, provided that the mass spectrum is quantized as

$$M_n^2 = \frac{4r_0^2}{R^4} n(n+1) , \quad n = 1, 2, \dots . \quad (54)$$

In that case $Y(z) \sim P_{n-1}^{(2,0)}(z)$ in the standard notation of [16]. Hence, the mass gap must be of the order of the mass associated with the lowest eigenvalue $n = 1$, which gives a mass gap $M_{\text{gap}} \sim \frac{r_0}{R^2}$.

In the rest of this subsection we study the potentials arising from two different trajectories.

3.2.1 Case I:

For the trajectory passing through the centre of the 3-sphere we set

$$x_5 = x_6 = 0 , \quad u = 0 . \quad (55)$$

We have

$$f(U) = U^2(U^2 - r_0^2) , \quad g(U) = 1 \quad (56)$$

and $U_{\text{min}} = r_0$. Then the expression for the length and the potential as functions of U_0 are given by (we change the integration variable in (6) and (7) as $\rho = U^2$):

$$\begin{aligned} L &= R^2 U_0 \sqrt{U_0^2 - r_0^2} \int_{U_0^2}^{\infty} \frac{d\rho}{\rho \sqrt{(\rho - r_0^2)(\rho - U_0^2)(\rho + U_0^2 - r_0^2)}} \\ &= \frac{2R^2 U_0 k'}{U_0^2 - r_0^2} (\mathbf{\Pi}(k'^2, k) - \mathbf{K}(k)) , \end{aligned} \quad (57)$$

and

$$\begin{aligned}
E_{q\bar{q}} &= \frac{1}{2\pi} \int_{U_0^2}^{\infty} d\rho \left[\sqrt{\frac{\rho - r_0^2}{(\rho - U_0^2)(\rho + U_0^2 - r_0^2)}} - \frac{1}{\sqrt{\rho}} \right] - \frac{U_0 - r_0}{\pi} \\
&= \frac{\sqrt{2U_0^2 - r_0^2}}{\pi} (k'^2 \mathbf{K}(k) - \mathbf{E}(k)) + \frac{r_0}{\pi}, \tag{58}
\end{aligned}$$

where $k = \frac{U_0}{\sqrt{2U_0^2 - r_0^2}}$ and $k' = \sqrt{1 - k^2}$.

For $U_0 \gg \mu$ we have the usual Coulombic behaviour and the potential is given by (9). As U_0 decreases, for $U_0 \simeq 1.13r_0$ the length and energy reach their maximum values $L_{\max} = R^2/r_0$ and $E_{q\bar{q}}^{\max} \simeq 0.02r_0$. However, before that, for $U_0 \simeq 1.38r_0$, the energy turns positive and the corresponding value for the length is $L \simeq 0.88R^2/r_0$. As $U_0 \rightarrow r_0$ we find that both the length and the energy approach zero as

$$L \simeq \frac{\sqrt{2}R^2}{r_0} \sqrt{\frac{U_0}{r_0} - 1} \left(\ln \left(\frac{8r_0}{U_0 - r_0} \right) - 2 \right) \tag{59}$$

and

$$E_{q\bar{q}} \simeq \frac{U_0 - r_0}{2\pi} \left(\ln \left(\frac{8r_0}{U_0 - r_0} \right) - 3 \right). \tag{60}$$

The plots of the length and potential as a function of U_0 and that of the potential as a function of the length are given by curve (a) in figs. 2, 3 and 4. We see that the behaviour is similar to the case of finite temperature, but zero rotation parameter.

3.2.2 Case II:

For the trajectory with

$$x_1 = x_2 = x_3 = x_4 = 0, \quad U = u, \tag{61}$$

we have

$$f(U) = (U^2 + r_0^2)^2, \quad g(U) = 1 \tag{62}$$

and that $U_{\min} = 0$. The expressions for the length and the potential as functions of U_0 are given by (again we change the integration variable in (6) and (7) as $\rho = U^2$):

$$\begin{aligned}
L &= R^2(U_0^2 + r_0^2) \int_{U_0^2}^{\infty} \frac{d\rho}{(\rho + r_0^2) \sqrt{\rho(\rho - U_0^2)(\rho + U_0^2 + 2r_0^2)}} \\
&= \frac{\sqrt{2}R^2}{\sqrt{U_0^2 + r_0^2}} \left(\mathbf{\Pi} \left(\frac{1}{2}, k \right) - \mathbf{K}(k) \right) \tag{63}
\end{aligned}$$

and

$$\begin{aligned}
E_{q\bar{q}} &= \frac{1}{2\pi} \int_{U_0^2}^{\infty} d\rho \left(\frac{\rho + r_0^2}{\sqrt{\rho(\rho - U_0^2)(\rho + U_0^2 + 2r_0^2)}} - \frac{1}{\sqrt{\rho}} \right) - \frac{U_0}{\pi} \\
&= \frac{\sqrt{U_0^2 + r_0^2}}{\sqrt{2}\pi} \left(\mathbf{K}(k) - 2\mathbf{E}(k) \right), \tag{64}
\end{aligned}$$

where $k = \sqrt{\frac{U_0^2 + 2r_0^2}{2(U_0^2 + r_0^2)}}$. We find that for $U_0 \rightarrow 0$

$$L \simeq \frac{\sqrt{2}R^2}{r_0} \left(\ln \left(\frac{4\sqrt{2}r_0}{U_0} \right) - \sqrt{2} \ln(1 + \sqrt{2}) \right) \quad (65)$$

and

$$E_{q\bar{q}} \simeq \frac{r_0}{\sqrt{2}\pi} \left(\ln \left(\frac{4\sqrt{2}r_0}{U_0} \right) - 2 \right). \quad (66)$$

Hence, we find the linear potential

$$E_{q\bar{q}} \simeq \frac{r_0^2}{2\pi R^2} L, \quad \text{for } L \gg \frac{R^2}{r_0}. \quad (67)$$

We note that the potential described by (63) and (64) is the same as that found in [22] using a two-centre metric, even though this is a different supergravity solution than (51).

The plot of the potential energy as a function of the quark–antiquark separation is given by curve (b) in fig. 5. Notice the smooth interpolation between the Coulombic and confining behaviours.

3.3 The general case

We would like to study the quark–antiquark potentials arising at general values of μ and r_0 from trajectories having different, nevertheless constant, values for the angle θ . Since there is an explicit dependence of the metric components on θ , consistency requires that the variation of the Nambu–Goto action with respect to θ is zero in order for the equations of motion to be obeyed. It is easy to see that this procedure allows $\theta = 0$ or $\theta = \pi/2$. There is no problem setting all the other angular variables to constants, since the metric components do not explicitly depend on them.

3.3.1 Trajectory with $\theta = 0$

In this case

$$f(U) = U^4 - r_0^2 U^2 - \mu^4, \quad g(U) = 1 \quad (68)$$

and the integrals for length and energy, given by (6) and (7) respectively, take the form

$$L = 2R^2 \sqrt{U_0^4 - r_0^2 U_0^2 - \mu^4} \int_{U_0}^{\infty} \frac{dU}{\sqrt{(U^4 - r_0^2 U^2 - \mu^4)(U^2 - U_0^2)(U^2 + U_0^2 - r_0^2)}}, \quad (69)$$

and

$$E_{q\bar{q}} = \frac{1}{\pi} \int_{U_0}^{\infty} dU \left[\sqrt{\frac{U^4 - r_0^2 U^2 - \mu^4}{(U^2 - U_0^2)(U^2 + U_0^2 - r_0^2)}} - 1 \right] - \frac{U_0 - U_H}{\pi}, \quad (70)$$

with $U_0 \geq U_{\min} = U_H$, where the location of the horizon is given in (42). For large U_0 the potential is, as usual, Coulombic, but there exists a maximal separation, as is

depicted in fig. 2 for various values of μ . At the values of U_0 where the separation is maximal, also the energy is maximal and always positive (fig. 3). This means that there is a screening behaviour because, once the potential turns positive, a configuration of two separate strings, each bounded by a circle in the Euclidean time direction, is energetically favoured and corresponds to a vanishing force between the charges. As $U_0 \rightarrow U_H$ we find that both the length and the energy approach zero as

$$L \simeq \sqrt{2}R^2(r_0^4 + 4\mu^4)^{-1/4} \sqrt{\frac{U_0}{U_H} - 1} \ln\left(\frac{U_H}{U_0 - U_H}\right) \quad (71)$$

and

$$E_{q\bar{q}} \simeq \frac{U_0 - U_H}{2\pi} \ln\left(\frac{U_H}{U_0 - U_H}\right). \quad (72)$$

The second branch of the potential, starting at the point of maximal separation and going to zero distance and zero energy, is unphysical for three reasons. First, since the energy on this branch is always positive the first branch is preferred, as it minimizes the energy. Second, it violates the concavity condition (11) (see also (79) below). Third, when $U_0 \rightarrow U_H$ the circumference of the string in the Euclidean direction becomes arbitrarily small in the region close to the horizon. Since the loop is contractible, the string can split into two strings, which have the shape of discs bounded by a circle. Therefore, the potential vanishes, which explains the screening when the two quarks are separated beyond the maximal distance.

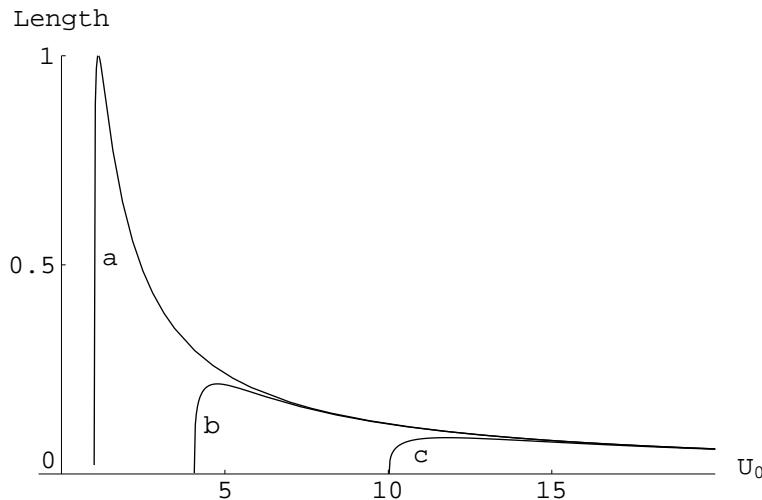


Figure 2: Curves (a), (b) and (c) correspond to the distance between a quark and an antiquark as a function of U_0 , as computed using (69) for three different values of $\mu = 0, 3$ and 10 , respectively. Lengths and energies are measured in units of $\frac{R^2}{r_0}$ and r_0 , respectively. All three curves approach $L = 0$ as $U_0 \rightarrow U_H$ according to (71). For large U_0 they unify according to (8) irrespectively of the value of μ . Curve (a) can be obtained using (57). Curve (c) is approximately what we would obtain using (46).

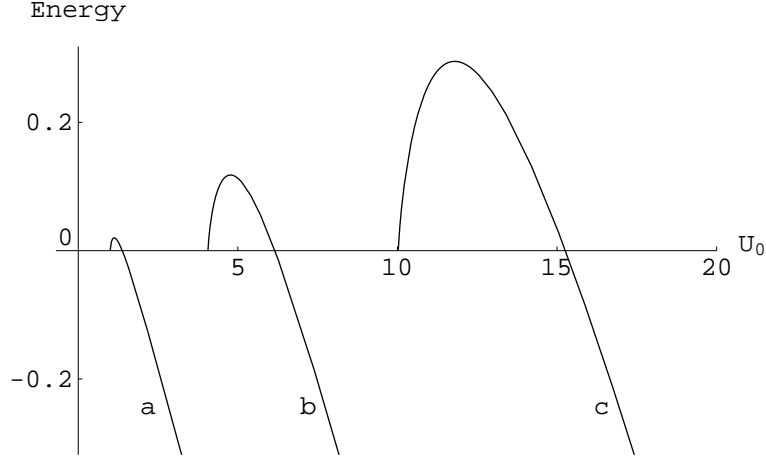


Figure 3: Curves (a), (b) and (c) correspond to the quark–antiquark potential as a function of U_0 as computed using (70) for three different values of $\mu = 0, 3$ and 10 , respectively. Energies are measured in units of r_0 . All three curves approach $U = 0$ as $U_0 \rightarrow U_H$ according to (72). For large U_0 the curves become parallel as they follow (9) with the energy shifted in its curve by $\frac{U_H}{\pi}$. Curve (a) can be obtained using (58). Curve (c) is approximately what we would obtain using (47).

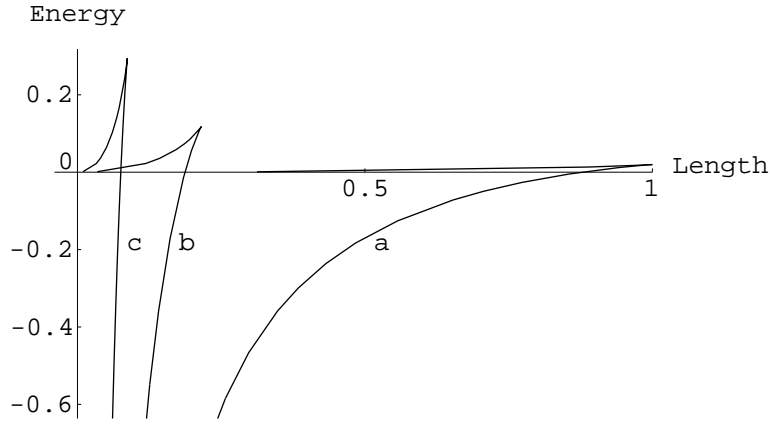


Figure 4: Curves (a), (b) and (c) correspond to the quark–antiquark potential as computed using (69) and (70) for the three different values of $\mu = 0, 3$ and 10 , respectively. Lengths and energies are measured in units of $\frac{R^2}{r_0}$ and r_0 , respectively. For small separations $L \rightarrow 0$, all three curves approach the Coulombic law. Curve (a) can be obtained using (57) and (58). Curve (c) is approximately what we would obtain using (46) and (47).

3.3.2 $\theta = \frac{\pi}{2}$

In this case we have

$$f(U) = U^4 - \mu^4, \quad g(U) = (U^4 - \mu^4)/(U^4 - r_0^2 U^2 - \mu^4). \quad (73)$$

The integrals for length and the potential energy are given by

$$L = 2R^2 \sqrt{U_0^4 - \mu^4} \int_{U_0}^{\infty} \frac{dU}{\sqrt{(U^4 - r_0^2 U^2 - \mu^4)(U^4 - U_0^4)}} \quad (74)$$

and

$$E_{q\bar{q}} = \frac{1}{\pi} \int_{U_0}^{\infty} dU \left[\frac{U^4 - \mu^4}{\sqrt{(U^4 - r_0^2 U^2 - \mu^4)(U^4 - U_0^2)}} - \sqrt{\frac{U^4 - \mu^4}{U^4 - r_0^2 U^2 - \mu^4}} \right] - \frac{1}{\pi} \int_{U_H}^{U_0} dU \sqrt{\frac{U^4 - \mu^4}{U^4 - r_0^2 U^2 - \mu^4}}, \quad (75)$$

where U_H is given by (42).⁸ As usual, the dependence of the potential energy for small separations L of the quark–antiquark (corresponding to large U_0) is Coulombic. For $U_0 \rightarrow U_H$ we have

$$L \simeq \frac{R^2 r_0}{\sqrt{2} U_H} (r_0^4 + 4\mu^4)^{-1/4} \ln \left(\frac{U_H}{U_0 - U_H} \right), \quad (76)$$

and

$$E_{q\bar{q}} \simeq \frac{r_0^2}{2\sqrt{2}\pi} (r_0^4 + 4\mu^4)^{-1/4} \ln \left(\frac{U_H}{U_0 - U_H} \right). \quad (77)$$

Eliminating U_0 we find a linear confining behaviour

$$E_{q\bar{q}} \simeq \frac{r_0 U_H}{2\pi R^2} L, \quad \text{for } L \gg \frac{R^2 r_0}{U_H} (r_0^4 + 4\mu^4)^{-1/4}. \quad (78)$$

However, for intermediate values of the separation, the behaviour of the system depends crucially on the value of the ratio $\lambda = \frac{\mu}{r_0}$. There is a critical value $\lambda_{\text{cr}} \simeq 2.85$ such that for $\lambda < \lambda_{\text{cr}}$ the behaviour is qualitatively the same as in the case $\mu = 0$ that we have already examined (see curve (a) in fig. 5).

However, for $\lambda > \lambda_{\text{cr}}$ the behaviour is different and resembles the situation occurring in first order phase transitions in statistical systems.⁹ We describe the situation below and we also refer to figs. 6 and 7 for graphical details of the length as a function of U_0 and of the potential energy as a function of the length. In particular, there are three different branches corresponding to the segments ABCDEF, FJKLM and MNOPQRS. For large U_0 , equivalently small L , we have the usual Coulombic behaviour given by (9) (point A in figs. 6 and 7). As we lower U_0 , we see that for all points until point B there is a unique value for U_0 , that is a unique trajectory, corresponding to each value for the length. At point B two different values of U_0 correspond to the same value for the length

⁸For $\mu = 0$ both (74) and (75) tend to the integrals in (63) and (64) after we change variables $U^2 \rightarrow U^2 + r_0^2$ and rename $U_0^2 \rightarrow U_0^2 + r_0^2$.

⁹In terms of thermodynamic quantities, our L , $E_{q\bar{q}}$ and U_0 correspond to pressure, Gibbs potential and volume, respectively. At $\lambda = \lambda_{\text{cr}}$ the first order phase transition degenerates to a second order one. Then U_0 plays the rôle of an order parameter. For details on the related statistical and thermodynamical aspects, see, for instance, [23].

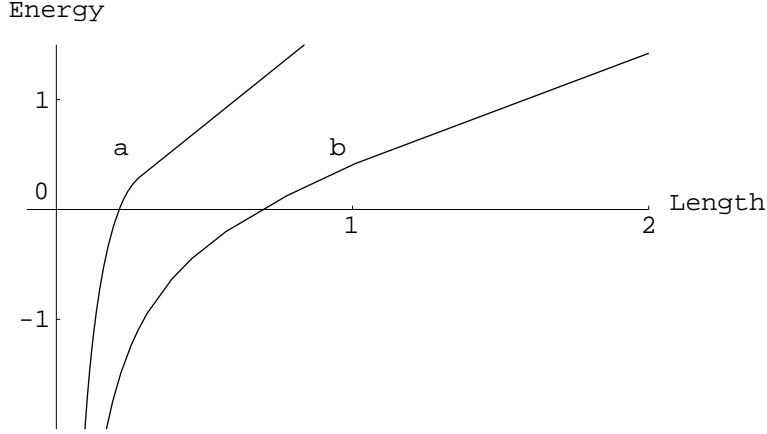


Figure 5: Curves (a), (b) correspond to the quark–antiquark potential as computed using (74) and (75) for the two different values of $\mu = 2$ and 0 , respectively, corresponding to $\lambda < \lambda_{\text{cr}} \simeq 2.85$. Lengths and energies are measured in units of $\frac{R^2}{r_0}$ and r_0 , respectively. For small separation $L \rightarrow 0$, both curves approach the Coulombic law. For large separation we obtain a linear behaviour. Curve (b) can also be obtained using (63) and (64).

(the other point is M) and after that, up to point D, there are three different U_0 's for each value of the length (for instance, C, N and L). Note also that in the entire path ABCD the energy is the smallest compared with the points on the other two branches that have the same length. When the unique point D is reached, the energy-surface intersects itself and after that the energy minimum comes from the other branch of the curve. Hence, all three points Q, E and J have the same length, but the physical state corresponds to point Q since this has the smallest energy of the three. Therefore, we conclude that the physical path is not the one joining the points ADFKMOS but rather ABCDOQRS, where the energy is always a minimum for a given value of the length. Hence, the entire branch FJKLM connecting the two extrema F and M is unphysical. There is an additional reason why this branch is not part of a physical path, namely that the concavity condition for the potential (11) is violated there. This is easily seen by first finding the behaviour close to the two extrema marked by F and M. Using (12) and (13) we find that close to a maximum F

$$E_{q\bar{q}} - E_{q\bar{q}}^{\text{max}} \simeq \frac{\sqrt{f(U_0^{\text{max}})}}{2\pi R^2} (L_{\text{max}} - L) [-1 \mp D_1(L_{\text{max}} - L)^{1/2}] , \quad (79)$$

where the minus (plus) sign corresponds to the branch BCDEF (FJKLM) and D_1 is a positive constant. Close to the minimum M, the corresponding expansion is

$$E_{q\bar{q}} - E_{q\bar{q}}^{\text{min}} \simeq \frac{\sqrt{f(U_0^{\text{min}})}}{2\pi R^2} (L - L_{\text{min}}) [1 \mp D_2(L - L_{\text{min}})^{1/2}] , \quad (80)$$

where now the minus (plus) sign corresponds to the branch MNOQR (FJKLM) and D_2 is another positive constant. We see that the concavity condition (13) is violated in the branch FJKLM. In contrast, in the entire physical path ABCDOQRS this condition is

preserved. Note also that exactly at the critical value $\lambda = \lambda_{\text{cr}} \simeq 2.85$ the first order degenerates to a second order phase transition. Then using the fact that not only the first but also the second derivative of the length vanishes at some critical value U_0^{cr} we find that

$$E_{q\bar{q}} - E_{q\bar{q}}^{\text{cr}} \simeq \frac{\sqrt{f(U_0^{\text{cr}})}}{2\pi R^2} (L - L_{\text{cr}}) (1 - D_3 |L - L_{\text{cr}}|^{1/3}) , \quad (81)$$

for some constant D_3 . Therefore, using (12), we find that $L - L_{\text{cr}} \sim (U_0 - U_0^{\text{cr}})^3$. It can also be shown that $U_0 - U_0^{\text{cr}} \sim \lambda - \lambda_{\text{cr}}$ for $\lambda > \lambda_{\text{cr}}$ and of course it vanishes, as usual for an order parameter, for $\lambda < \lambda_{\text{cr}}$. Hence, the corresponding critical exponents take the classical values 3 and 1.

Finally, we want to comment on the confining behaviour for large quark–antiquark separation, present for all values of μ and r_0 , which is somewhat unexpected. Once the potential becomes positive, a configuration of two separate worldsheets is energetically preferred. The breaking of the tube–like worldsheet connecting the quark–antiquark pair is possible, if the proper length of the circle $\sqrt{g_{\tau\tau}}/T_H \sim \sqrt{\alpha'}$ as the string approaches the horizon. Using our metric (40) we find that a breaking of the string is likely when either $\mu \gtrsim \sqrt{R}r_0$ or $r_0 \gtrsim \sqrt{R}\mu$ and in these cases one has screening as in the case of $\theta = 0$. On the other hand, for $r_0 \sim \mu$, the circumference $\sim \sqrt{\alpha'}R$ is quite large and the worldsheets on the confining branch of the potential are stable, although its energy is larger than that of two disconnected worldsheets. The answer to this problem might be related to the discussion in [22], where an (unexpected) linear potential was found to be unstable because of extra QCD states.

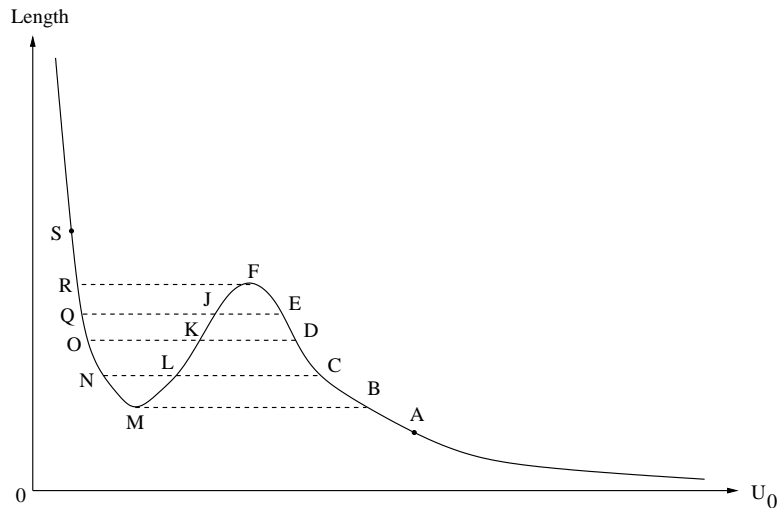


Figure 6: The quark–antiquark separation, as computed using (74) for $\lambda > \lambda_{\text{cr}} \simeq 2.85$.

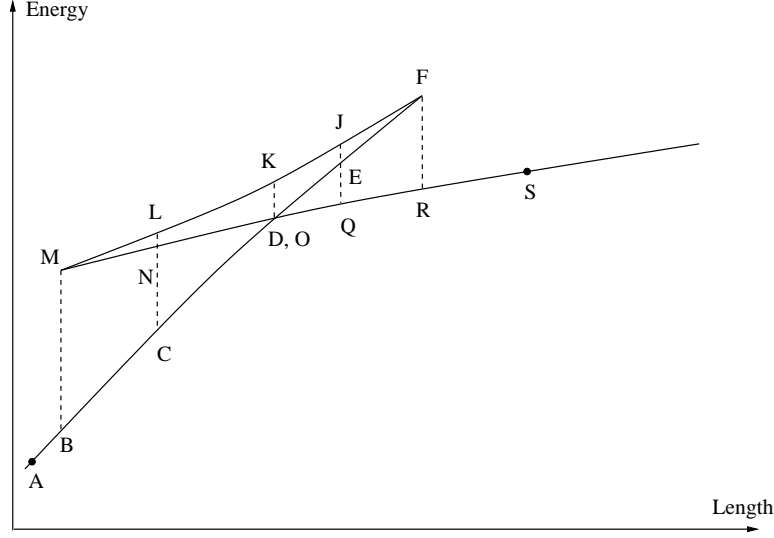


Figure 7: The quark–antiquark potential as a function of the separation, as computed using (74) and (75) for $\lambda > \lambda_{\text{cr}} \simeq 2.85$.

4 Rotating D3-brane for YM in three dimensions

Models of YM theories in 2+1 dimensions at zero temperature can be constructed, using non-extremal D3-branes, by compactifying the Euclidean time direction on a circle of circumference $\beta = 1/T_{\text{H}}$ [19, 24]. An extension of this model, where there is a clear decoupling of the Kaluza–Klein modes associated with the Euclidean time compared with the modes that have vanishing Kaluza–Klein charge, is based on rotating D3-branes [5, 25, 7]. The space–space Wilson loop for the zero-rotation case has been computed in [26].

As before, setting all the angles to constants in searching for trajectories is consistent with the equations of motion only in the cases $\theta = 0$ or $\theta = \frac{\pi}{2}$.

4.1 $\theta = 0$

In this case we have

$$f(U) = U^2(U^2 - r_0^2), \quad g(U) = \frac{U^2(U^2 - r_0^2)}{U^4 - r_0^2 U^2 - \mu^4}. \quad (82)$$

Then the integrals for the length and the energy, given by (6) and (7) respectively, take the form

$$L = 2R^2 \sqrt{U_0^2(U_0^2 - r_0^2)} \int_{U_0}^{\infty} \frac{dU}{\sqrt{(U^4 - r_0^2 U^2 - \mu^4)(U^2 - U_0^2)(U^2 + U_0^2 - r_0^2)}}, \quad (83)$$

and

$$E_{q\bar{q}} = \frac{1}{\pi} \int_{U_0}^{\infty} dU \left[\frac{U^2(U^2 - r_0^2)}{\sqrt{(U^4 - r_0^2 U^2 - \mu^4)(U^2 - U_0^2)(U^2 + U_0^2 - r_0^2)}} - \sqrt{\frac{U^2(U^2 - r_0^2)}{U^4 - r_0^2 U^2 - \mu^4}} \right] - \frac{1}{\pi} \int_{U_H}^{U_0} dU \sqrt{\frac{U^2(U^2 - r_0^2)}{U^4 - r_0^2 U^2 - \mu^4}} , \quad (84)$$

with U_H as given by (42). For small distances we have, as usual, a Coulombic behaviour for the potential, whereas we find, as $U_0 \rightarrow U_H$, a linear behaviour since

$$L \simeq R^2 \frac{\mu^2}{U_H} (r_0^4 + 4\mu^4)^{-1/2} \ln \left(\frac{U_H}{U_0 - U_H} \right) \quad (85)$$

and

$$E_{q\bar{q}} \simeq \frac{\mu^4}{2\pi U_H} (r_0^4 + 4\mu^4)^{-1/2} \ln \left(\frac{U_H}{U_0 - U_H} \right) \simeq \frac{\mu^2}{2\pi R^2} L , \quad \text{for } L \gg \frac{R^2 \mu^2}{U_H} (r_0^4 + 4\mu^4)^{-1/2} . \quad (86)$$

Similar to what we have already encountered in section 3, there exists a critical value $\lambda_{\text{cr}} \simeq 0.46$ for the ratio $\lambda = \frac{\mu}{r_0}$, such that for $\lambda > \lambda_{\text{cr}}$ the behaviour goes smoothly from Coulombic to confining. However, for $\lambda = \lambda_{\text{cr}}$ there is a second order phase transition and for $\lambda < \lambda_{\text{cr}}$ the behaviour differs and resembles the one depicted in figs. 6 and 7.

It is important to note here that this is not a transition from confinement to Coulombic potential in a three-dimensional theory, but in a four-dimensional theory on a circle. Only for large separation of the external charges is the theory effectively three-dimensional and do we observe confinement. But for small distances the string can probe the extra dimension and the Coulomb behaviour is that of the compactified four-dimensional theory.

4.2 $\theta = \frac{\pi}{2}$

In this case we have

$$f(U) = U^4 , \quad g(U) = \frac{U^4}{U^4 - r_0^2 U^2 - \mu^4} . \quad (87)$$

Then the integrals for the length and the potential energy are given by

$$L = 2R^2 U_0^2 \int_{U_0}^{\infty} \frac{dU}{\sqrt{(U^4 - r_0^2 U^2 - \mu^4)(U^4 - U_0^4)}} \quad (88)$$

and

$$E_{q\bar{q}} = \frac{1}{\pi} \int_{U_0}^{\infty} dU \left[\frac{U^4}{\sqrt{(U^4 - r_0^2 U^2 - \mu^4)(U^4 - U_0^4)}} - \frac{U^2}{\sqrt{U^4 - r_0^2 U^2 - \mu^4}} \right] - \frac{1}{\pi} \int_{U_H}^{U_0} dU \frac{U^2}{\sqrt{U^4 - r_0^2 U^2 - \mu^4}} , \quad (89)$$

where U_H is given by (42). The behaviour is Coulombic for small separations and confining for $U_0 \rightarrow U_H$, since we then have

$$L \simeq \frac{R^2}{\sqrt{2}}(r_0^4 + 4\mu^4)^{-1/4} \ln \left(\frac{U_H}{U_0 - U_H} \right), \quad (90)$$

and

$$\begin{aligned} E_{q\bar{q}} &\simeq \frac{U_H^2}{2\sqrt{2}\pi}(r_0^4 + 4\mu^4)^{-1/4} \ln \left(\frac{U_H}{U_0 - U_H} \right) \\ &\simeq \frac{U_H^2}{2\pi R^2} L, \quad \text{for } L \gg R^2(r_0^4 + 4\mu^4)^{-1/4}. \end{aligned} \quad (91)$$

As in section 4.1 we found a transition from confinement to the Coulomb law, but the force between the external charges is a smooth function of L . Also in this case the comments made in the last paragraph of section 4.1 apply.

5 Concluding remarks and some open problems

We have studied Wilson loops and computed the associated heavy quark–antiquark potential within the AdS/CFT correspondence and in the supergravity approximation.

We have studied four-dimensional supersymmetric gauge theories at zero temperature with broken gauge symmetry, using multicentre D3-brane solutions. In this case we found that there is a complete screening of charges that we attributed to the existence of a mass gap in the gauge theory. It is very important to understand such a mass gap from a field theoretical point of view. A first difficulty is that the mass gap, and in fact all interesting phenomena, occur at a scale $\sim \frac{r_0}{R^2}$, whereas the vev masses $\sim r_0$ are much larger. This has a similarity with the fact that two different energy scales occur in the AdS/CFT correspondence [27]. It is also important to understand to what extent our results are a feature of the continuum nature of the brane distribution.

Gauge theories at finite temperature were also studied using rotating D3-brane solutions. In this case we found two distinct classes of potentials. One is similar to that obtained by using non-extremal D3-branes with zero rotation and the other to one that interpolates between a Coulombic and a confining potential. In the latter case, depending on the ratio of the extremality to the rotation parameter, the interpolation is smooth or the transition between the two regions is reminiscent of phase transitions in statistical systems. The potential contains three distinct branches, one of which violates the concavity condition that states that the force between a quark and an antiquark is a monotonously decreasing function of their separation. However, the physical path, similarly to the physical isotherm in statistical systems, connects the Coulombic and the confining regions of the potential through the coexistence point, where the potential is smooth, but the force is discontinuous. It would be extremely interesting to understand this discontinuity from a field theory point of view. Using the same rotating brane solution, non-supersymmetric three-dimensional gauge theories at zero temperature were

also studied by computing the heavy quark–antiquark potentials from the associated space–space Wilson loops, yielding similar results.

There are several straightforward, but quite important, generalizations of our work. The first is to study the potentials arising from the most general rotating D3-brane solution [4, 6, 7] (eq. (30) in [7]), which contains three rotational parameters. It can be easily seen that there exist trajectories with all the angles corresponding to S^5 fixed. Second, it will be interesting to compute the heavy quark–antiquark potential from the space–space Wilson loop obtained by using the rotating D4-brane solution of [28]. This is appropriate for studying, in the present context, four-dimensional non-supersymmetric gauge theories at zero temperature. Finally, we mention that a concavity condition for Wilson loops, generalizing (11), has been derived [29] for the cases in which there is a relative orientation between the quark and antiquark with respect to the sphere coordinates. The prototype computation of such potentials was done, for the case of the $AdS_5 \times S^5$ background, in [10], and it indeed obeys the condition of [29]. In that respect it is important to know if this generalized concavity condition is obeyed by the similar potentials one would obtain using rotating D3-brane metrics.

Another important line of research concerns the inclusion of corrections to the leading order supergravity approximation. It would be interesting to include α' -corrections to the supergravity backgrounds and to study how they affect our solution. Note that such corrections are always present for the $N = 4$ theory on the Coulomb branch, since the Weyl tensor does not vanish and the Gross–Witten term in the supergravity action is non-zero. Only at the origin of the Coulomb branch is the Weyl tensor exactly zero and $AdS_5 \times S^5$ an exact background of type IIB string theory. Although a complete formulation of string theory in the background of Ramond fields is still missing, it would also be interesting to calculate corrections due to worldsheet fluctuations. This could be done, for instance, using a Green–Schwarz formulation and expanding around the classical configuration. Calculations of this kind have recently been performed in [30].

A D3-branes distributed on a ring

In this appendix we compute the quark–antiquark potential for N branes distributed, uniformly in the angular direction, around the circumference of a ring of radius r_0 in the x_5 – x_6 plane [8]. Their centres are given by

$$\begin{aligned} \mathbf{x}_i &= (0, 0, 0, 0, r_0 \cos \phi_i, r_0 \sin \phi_i) , \\ \phi_i &= \frac{2\pi i}{N} , \quad i = 0, 1, \dots, N . \end{aligned} \tag{A.1}$$

In the near–horizon limit the harmonic function is given by

$$\begin{aligned} H &= \frac{R^4}{\alpha'^2} \frac{U^2 + r_0^2}{[(U^2 + r_0^2)^2 - 4r_0^2 u^2]^{3/2}} \Sigma_N(x, \psi) , \\ U^2 &= U_1^2 + \dots + U_6^2 , \quad u^2 = U_5^2 + U_6^2 . \end{aligned} \tag{A.2}$$

where

$$\Sigma_N(x, \psi) \equiv \frac{\sinh(Nx)}{\cosh(Nx) - \cos(N\psi)} + N \frac{\left((U^2 + r_0^2)^2 - 4r_0^2 u^2 \right)^{1/2}}{U^2 + r_0^2} \frac{\cosh Nx \cos N\psi - 1}{(\cosh Nx - \cos N\psi)^2}. \quad (\text{A.3})$$

The variable x appearing in (A.3) is defined as

$$e^x \equiv \frac{U^2 + r_0^2}{2r_0 u} + \sqrt{\left(\frac{U^2 + r_0^2}{2r_0 u} \right)^2 - 1}, \quad (\text{A.4})$$

whereas ψ is the angular variable in the x_5 - x_6 plane. In the limit of a continuous distribution of branes where $N \gg 1$, we may set Σ_N equal to 1. This is a very good approximation unless we approach the ring at $U = u = r_0$ down to distances such that $U/r_0 - 1 = \mathcal{O}(\frac{1}{N})$ or smaller.

We studied two kinds of trajectories, one where the trajectory is orthogonal to the plane in which the ring is lying, i.e. $u = 0$, and one where the trajectory runs in a radial direction in the plane of the ring towards the centre of the ring, i.e. $U = u$. In the first case we find (without setting in (A.2) $\Sigma_N = 1$) for $f(U)$ and $g(U)$ the same functions as in (62). Hence, the corresponding quark-antiquark potential is the same as the one computed in section 3.2.2. In the second case we consider only the continuum limit, where $\Sigma_N = 1$. We have

$$f(U) = \frac{(U^2 - r_0^2)^3}{(U^2 + r_0^2)}, \quad g(U) = 1 \quad (\text{A.5})$$

and $U_{\min} = r_0$. After we change variables as $\rho = U^2$, we obtain for the length and the energy the integrals

$$L = R^2 (U_0^2 - r_0^2)^{3/2} \int_{U_0^2}^{\infty} \frac{d\rho (\rho + r_0^2)}{\sqrt{\rho(\rho - r_0^2)^3 [(\rho - r_0^2)^3 (U_0^2 + r_0^2) - (\rho + r_0^2)(U_0^2 - r_0^2)^3]}} \quad (\text{A.6})$$

and

$$E_{q\bar{q}} = \frac{1}{2\pi} \int_{U_0^2}^{\infty} d\rho \left\{ \frac{\sqrt{U_0^2 + r_0^2} (\rho - r_0^2)^{3/2}}{\sqrt{\rho [(\rho - r_0^2)^3 (U_0^2 + r_0^2) - (\rho + r_0^2)(U_0^2 - r_0^2)^3]}} - \frac{1}{\sqrt{\rho}} \right\} - \frac{U_0 - r_0}{\pi}. \quad (\text{A.7})$$

For $U_0 \gg r_0$ the potential is Coulombic and has the same form as in (9). In contrast to the previous trajectory, we do not find confinement for $U_0 \simeq r_0$. We approximately evaluated the behaviour for $U_0 \simeq r_0$. The result is

$$L \simeq \frac{2\sqrt{\pi}\Gamma(2/3)}{\Gamma(1/6)} \frac{R^2}{\sqrt{r_0(U_0 - r_0)}} \quad (\text{A.8})$$

and

$$E_{q\bar{q}} \simeq -\frac{\Gamma(2/3)}{\sqrt{\pi}\Gamma(1/6)} (U_0 - r_0). \quad (\text{A.9})$$

Therefore

$$E_{q\bar{q}} \simeq -4\sqrt{\pi} \left(\frac{\Gamma(2/3)}{\Gamma(1/6)} \right)^3 \frac{R^4}{r_0 L^2} . \quad (\text{A.10})$$

This can be interpreted as a screening of the L^{-1} Coulombic potential to an L^{-2} potential at large separation. The latter behaviour is characteristic of a quark–antiquark potential of a gauge theory living on D4-branes or on D3-branes smeared along a transverse direction. Indeed, for large L , when the corresponding trajectory approaches the ring circumference, it can be shown [8] that the supergravity solution becomes that of a D3-brane with a transverse direction smeared out. One finds that $f(U) = 4r_0 U^3$ and $g(U) = 1$. Then applying (6) and (7) we confirm (A.8)–(A.10).

Finally, let us mention that there is no known finite–temperature supergravity solution corresponding to the ring geometry for D3-branes. Owing to the no-hair theorem, the rotating D3-brane solutions are unique; in the supersymmetric limit, they give rise to a uniform distribution of D3-branes, in the case of one angular momentum, over a disc. The ring geometry arises naturally in the supersymmetric limit of rotating NS5- and D5-branes [31]. Then, the background corresponds to the exact conformal field theory coset model $SL(2, \mathbb{R})/U(1) \times SU(2)/U(1)$ [8, 31].

Acknowledgement

We would like to thank C. Bachas for a discussion. On the day we submitted our paper in hep-th we received [32] which has some overlap with sections 2 and 3.2 of our paper concerning complete screening in Wilson loops and mass gaps in the spectrum of gauge invariant operators in backgrounds corresponding to continuous distributions of D3-branes.

References

- [1] J. Maldacena, *Adv. Theor. Math. Phys.* **2** (1998) 231, hep-th/9711200.
- [2] S.S. Gubser, I.R. Klebanov and A.M. Polyakov, *Phys. Lett.* **B428** (1998) 105, hep-th/9802109.
- [3] E. Witten, *Adv. Theor. Math. Phys.* **2** (1998) 253, hep-th/9802150.
- [4] M. Cvetič and D. Youm, *Nucl. Phys.* **B477** (1996) 449, hep-th/9605051.
- [5] J.G. Russo, *Nucl. Phys.* **B543** (1999) 183, hep-th/9808117.
- [6] P. Kraus, F. Larsen and S.P. Trivedi, *JHEP* **03** (1999) 003, hep-th/9811120.
- [7] J.G. Russo and K. Sfetsos, *Adv. Theor. Math. Phys.* **3** (1999) 131, hep-th/9901056.
- [8] K. Sfetsos, *JHEP* **01** (1999) 015, hep-th/9811167.

- [9] S. Rey and J. Yee, *Macroscopic strings as heavy quarks in large N gauge theory and Anti-de-Sitter supergravity*, hep-th/9803001.
- [10] J. Maldacena, Phys. Rev. Lett. **80** (1998) 4859, hep-th/9803002.
- [11] C. Bachas, Phys. Rev. **D33** (1986) 2723.
- [12] B. Baumgartner, H. Grosse and A. Martin, Nucl. Phys. **B254** (1985) 528.
- [13] Y. Kinar, E. Schreiber and J. Sonnenschein, *Q anti- Q potential from strings in curved space-time: Classical results*, hep-th/9811192.
- [14] S. Rey, S. Theisen and J. Yee, Nucl. Phys. **B527** (1998) 171 hep-th/9803135.
- [15] A. Brandhuber, N. Itzhaki, J. Sonnenschein and S. Yankielowicz, Phys. Lett. **B434** (1998) 36, hep-th/9803137.
- [16] I.S. Gradshteyn and I.M. Ryzhik, *Table of integrals, series and products*, fifth edition (Academic Press, New York, 1994).
- [17] P. Byrd and M. Friedman, *Handbook of Elliptic Integrals for Engineers and Physicists*, second edition, (Springer Verlag, Heidelberg, 1971).
- [18] A. Kehagias and K. Sfetsos, Phys. Lett. **B454** (1999) 270, hep-th/9902125.
- [19] E. Witten, Adv. Theor. Math. Phys. **2** (1998) 505, hep-th/9803131.
- [20] M. Abramowitz and I.A. Stegun, *Handbook of mathematical functions*, (Dover Publications, New York, 1964).
- [21] B. Svetitsky, Phys. Rep. **132** (1986) 1.
- [22] J.A. Minahan and N.P. Warner, JHEP **06** (1998) 005, hep-th/9805104.
- [23] H.B. Callen, *Thermodynamics and introduction to thermostatistics*, 2nd edition, (John Wiley & Sons, New York, 1985).
- [24] C. Csáki, H. Ooguri, Y. Oz and J. Terning, JHEP **01** (1999) 017, hep-th/9806021;
R. de Mello Koch, A. Jevicki, M. Mihailescu and J. Nunes, Phys. Rev. **D58** (1998) 105009, hep-th/9806125;
M. Zyskin, Phys. Lett. **B439** (1998) 373, hep-th/9806128.
- [25] C. Csáki, Y. Oz, J.G. Russo and J. Terning, Phys. Rev. **D59** (1999) 065008, hep-th/9810186.
- [26] A. Brandhuber, N. Itzhaki, J. Sonnenschein and S. Yankielowicz, JHEP **06** (1998) 001, hep-th/9803263.
- [27] A.W. Peet and J. Polchinski, Phys. Rev. **D59** (1999) 065011.

- [28] C. Csaki, J.G. Russo, K. Sfetsos and J. Terning, Phys. Rev. **D60** (1999) 044001, hep-th/9902067.
- [29] H. Dorn and V.D. Pershin, Phys. Lett. **B461** (1999) 338, hep-th/9906073.
- [30] J. Greensite and P. Olesen, JHEP **04** (1999) 001, hep-th/9901057;
S. Forste, D. Ghoshal and S. Theisen, JHEP **08** (1999) 013, hep-th/9903042;
S. Naik, Phys. Lett. **B464** (1999) 73, hep-th/9904147.
- [31] K. Sfetsos, *Rotating NS5-brane solution and its exact string theoretical description*, Proceedings of the *32nd International Symposium Ahrenshoop on the Theory of Elementary Particles*, Buckow, Germany, 1-5 September 1998, hep-th/9903201.
- [32] D.Z. Freedman, S.S. Gubser, K. Pilch and N.P. Warner, *Continuous distributions of D3-branes and gauged supergravity*, hep-th/9906194.